

# Spectral Sensitivity of Sensors for a Color-Image Descriptor Invariant to Changes in Daylight Conditions

Javier Romero,\* Javier Hernández-Andrés,  
Juan Luis Nieves, Eva M. Valero

Departamento de Óptica, Facultad de Ciencias, Universidad de Granada, 18071 Granada, Spain

Received 22 June 2005; revised 13 December 2005; accepted 6 February 2006

*Abstract:* Previous authors (*J Opt Soc Am A* 2000; 17: 1952–1961; *J Opt Soc Am A* 2001; 18: 253–264) have proposed a pixel-by-pixel image descriptor that is invariant to certain changes in illumination. We have studied the possibility of applying such an invariant descriptor to scenery illuminated by natural light, by choosing sensors that allow the invariant to behave satisfactorily under daylight. We obtained different triads of monochromatic sensors by using an exhaustive-search method and compared the results with those obtained with other triads proposed by different authors. We extended our study to Gaussian sensors centered in the wavelengths considered for the monochromatic sensors and to commercial CCD camera sensors. Satisfactory results are achieved for Gaussian sensors with maximum sensitivities at different locations. © 2006 Wiley Periodicals, Inc. *Col Res Appl*, 31, 391–398, 2006; Published online in Wiley InterScience (www.interscience.wiley.com). DOI 10.1002/col.20243

*Key words:* sensors; color invariant; daylight; color constancy

## INTRODUCTION

From a strictly colorimetric point of view, the color of an object in a scene depends both upon the spectral composition of the light that illuminates the object and the object's spectral reflectance. As far as the perceived color of the object is concerned, we must also take into consideration the distribution of color in its surrounding environment and the

adaptation conditions of the observer. If the light source that illuminates the scene changes, the measured color of the object also changes, but the color perceived by the observer may remain unchanged if the right conditions prevail to stimulate the capacity of the visual system to maintain the appearance of an object's color whatever the light it receives. This phenomenon is known as color constancy and it is the coveted goal of researchers in the field of artificial vision to find a way to imbue object-recognition systems with the capacity of the human visual system to transform the image of a scene in such a way that it remains the same whatever the changes in illuminant.

Marchant and Onyango<sup>1</sup> and Finlayson and Hordley<sup>2</sup> defined an invariant in each pixel of an image, the calculation of which only requires the R, G, and B values of the pixel itself. According to their method, the color image can be translated into a grey-scale image, in each pixel of which the level of grey represents the value of the invariant parameter, which remains the same whatever the illumination of the scene. With this definition of the invariant parameter, color constancy can be fully achieved if the illuminant is Planckian and the three sensors that capture the image have Dirac's  $\delta$ -type sensitivities.<sup>2</sup> These two conditions are the ideal ones. The application of the invariant will depend upon the extent to which the real illuminants that resemble Planckian ones and the sensors of the camera, of more-or-less wide spectral sensitivity, can provide results that are not far removed from those that the ideal monochromatic sensors give.

Finlayson and Hordley<sup>2</sup> argue that the chromaticity coordinates of most illuminants, whether they be daylight or artificial (halogen or fluorescent), are close to the locus of the blackbody in the CIE 1931 chromaticity diagram. Nevertheless, because of metamerism, an illuminant may have

\*Correspondence to: Javier Romero (e-mail: jromero@ugr.es)

Contract grant sponsor: Comisión Interministerial de Ciencia y Tecnología (CICYT), Spain, Contract grant number: DPI 2004–03734.  
© 2006 Wiley Periodicals, Inc.

quite a different relative spectral composition from that of the Planckian one at the same color temperature. These differences in spectral composition may determine the applicability of the invariant, particularly when the sensors used are either narrow-band or monochromatic.

Marchant and Onyango<sup>3,4</sup> widened their proposed invariant to include daylight. Their method is based on the possibility of expressing the logarithm of the spectral power distribution (SPD) of daylight in terms of a linear model with only one degree of freedom. To do this they made a principal component analysis (PCA) of the logarithms of nine daylight SPDs with color temperatures of between 4000 and 20 000 K at intervals of 2000 K, arrived at by the CIE method.<sup>5</sup> These authors represent daylight by resorting to the mean vector and first eigenvector of the linear basis. To represent daylight the CIE recommends using the mean vector plus two eigenvectors.<sup>6</sup> Other authors,<sup>7-9</sup> however, believe that a larger dimension is required when dealing with bases constructed from experimental measurements of daylight obtained under a wide range of atmospheric conditions.

As far as monochromatic sensors are concerned, Finlayson and Hordley<sup>2</sup> analyzed the behavior of three such sensors with their sensitivities located at the wavelengths 450, 540, and 610 nm. In another work, Finlayson<sup>10</sup> found that narrow-band sensors centered on these wavelengths afforded a clearer understanding of metamerism, chromatic adaptation, and color processing. Marchant and Onyango<sup>1</sup> based their choice of wavelengths (440.8, 530.5, and 605.2 nm) upon a calculation of the central wavelengths of a commercial CCD camera. In a later work<sup>4</sup> they studied triads of sensors centered on wavelengths, of which one was variable and the other two fixed at the ends of the visible spectrum. Their study<sup>4</sup> was focused upon the viability of their mathematical representation of daylight for the use of the invariant, but they did not specify which set of sensors would provide the best results in recognizing objects under these illumination conditions.

By using wide-band sensors corresponding to those of commercial CCD cameras and applying their invariant, Marchant and Onyango<sup>1</sup> satisfactorily classified vegetation against soil in images taken under daylight. Finlayson and Hordley<sup>2</sup> studied the inherent difficulties in obtaining invariant images when using real sensors, despite which they got good results in an object-recognition experiment. Various other authors<sup>11-13</sup> have used diverse techniques to improve on these results using real sensors, among which is that of applying spectral sharpening to the spectral sensitivity of the sensors. This technique<sup>11</sup> permits the transformation of the sensitivities to others which capture most of the information taken by the original ones, but being narrower, are closer to the requirements of the exact definition of the invariant.

In this work we have studied two aspects of the definition of the invariant proposed by Marchant and Onyango<sup>1</sup> and Finlayson and Hordley.<sup>2</sup> The first of these was the possibility of applying the invariant to images of scenes taken in daylight with different color temperatures. To this end we used a basis obtained from wide sets of experimental mea-

surements taken over all four seasons and at all times of the day.<sup>9</sup> We have repeated the calculations made by Marchant and Onyango<sup>1,4</sup> but using a set of 2600 daylight experimental measurements to obtain that of the linear model by PCA, instead of the nine daylight SPD determined by the CIE method.

The second problem to address was the choice of optimum sensors to be used in the definition of the invariant. With images taken under natural light we studied the optimum location of the three wavelengths in the visible spectrum corresponding to the monochromatic sensors in the pixel-by-pixel definition of the invariant. As a previous step to real sensors, we studied the possibility of using sensors with a Gaussian profile centered on the predetermined wavelengths. These sensors may have great spectral similarity to those used in commercial digital cameras.<sup>14</sup> After this we used the sensors of a commercial CCD camera and compared the results with those obtained with Gaussian sensors and those deriving from the application of spectral-sharpening techniques.<sup>2,11</sup> By analyzing images of natural scenes and calculating the histograms generated by every illuminant of the scene, we tested the capacity of each set of sensors to capture images that were invariant to changes in illumination. We checked whether these could be superimposed upon each other or were shifted, thus impeding recognition of the objects in question.

#### DEFINITION OF THE INVARIANT

Taking three sensors with Dirac's  $\delta$ -type spectral sensitivity in the wavelengths  $\lambda_1$ ,  $\lambda_2$ , and  $\lambda_n$  the invariant is defined<sup>4</sup> as

$$F_{12} = y_{\lambda_1}/y_{\lambda_2}^{A_{12}} \quad (1)$$

where

$$y_{\lambda_1} = C_{\lambda_1}/C_{\lambda_1}; y_{\lambda_2} = C_{\lambda_2}/C_{\lambda_n} \quad (2)$$

$C_\lambda = g\rho(\lambda)E(\lambda)$  being the response of the sensor corresponding to the spectral radiance generated by the reflectance object  $\rho(\lambda)$  illuminated by the SPD  $E(\lambda)$ . The term  $g$  contains all the gain-factor components and those related to the geometry of the illumination.

If we are dealing with Planckian-type illuminants<sup>1</sup>:

$$A_{12} = \frac{1/\lambda_1 - 1/\lambda_n}{1/\lambda_2 - 1/\lambda_n} \quad (3)$$

The  $g$  term cancels in the calculation of  $y_{\lambda_1}y_{\lambda_2}$ , and then eliminating the dependence of the invariant with the illumination geometry. Moreover, as the coordinates  $y_{\lambda_1}y_{\lambda_2}$  are defined as ratios of the signals for two different sensors, the problem of having a high dynamic range in natural scenes due to shadows is removed. By applying the invariant to natural scenes we can obtain monochrome images where the shadows have been eliminated.<sup>3</sup>

If, however, we are dealing with daylight, Marchant and Onyango<sup>3,4</sup> state that this can be represented as

$$E(\lambda, T) = h(\lambda) \exp[u(\lambda)f(T)] \quad (4)$$

In this case  $A_{12}$  is defined as

$$A_{12} = \frac{u(\lambda_1) - u(\lambda_n)}{u(\lambda_2) - u(\lambda_n)} \quad (5)$$

In Eq. (4)  $T$  is the correlated color temperature. For daylight to be expressed in this way it is sufficient that  $\ln E(\lambda)$  can be developed on a linear basis in the form of

$$\ln E(\lambda) = \ln h(\lambda) + u(\lambda)f(T) \quad (6)$$

That is to say, we can find via PCA a basis for the linear representation of a wide set of daylight data with different correlated color temperatures, in which  $\ln h(\lambda)$  is the mean vector and  $u(\lambda)$  the first eigenvector. The coefficient by which this eigenvector is multiplied depends upon color temperature alone and contains information about the different types of daylight illuminants.

The validity of the invariant defined in this way will depend therefore on whether Eq. (4) fulfills the spectral representation of daylight adequately and whether the hypothesis of narrow-band sensors can be applied. Whatever the case, if the sensors are real or broad band, the validity of the invariant for any set of objects can still be studied by drawing a graph<sup>2</sup> of logarithm  $y_{\lambda_2}$  versus logarithm  $y_{\lambda_1}$ , taking the values of  $C_\lambda$  to be the responses of the sensors with maximum sensitivity in the corresponding wavelength. If the invariant is valid for a set of sensors, this representation will produce dots that fall along a straight line for each object when it is illuminated with different illuminants, and the slope of this line,  $1/A_{12}$ , should be the same for all the objects.

### CALCULATION OF $A_{12}$

In a previous work<sup>9</sup> we have measured our own set of experimental daylight spectra consisting of 2600 SDPs between 380 and 780 nm at 5 nm intervals. These measurements were carried out over a period of 2 years in diverse meteorological conditions and at different times of day. By applying a PCA to this set of measurements, we obtained a linear representational basis for daylight which we felt allowed us to make a close enough spectral reconstruction of them for a dimension 5, that is, via the use of five vectors from the basis. This number is reduced to three when we try to satisfy purely colorimetric criteria.

In this work we have taken our experimental data set once more to apply a PCA to the logarithm of the values of  $E(\lambda)$  corresponding to daylight SPDs. In this way we were able to obtain a basis of eigenvectors which represented real daylight measurements. Marchant and Onyango<sup>3,4</sup> carried out a PCA on only nine SPDs, arrived at by the CIE method, at wavelength intervals of 10 nm. The nine SPDs had color temperatures of between 4000 and 20 000 K at intervals of 2000 K. It is easy to check in the CIE1931 chromaticity diagram that this choice does not result in uniformly spaced SPDs because to do this they should have taken color-temperature intervals measured in mireds. The reciprocal color-temperature scale, the unit of which is the mired, has

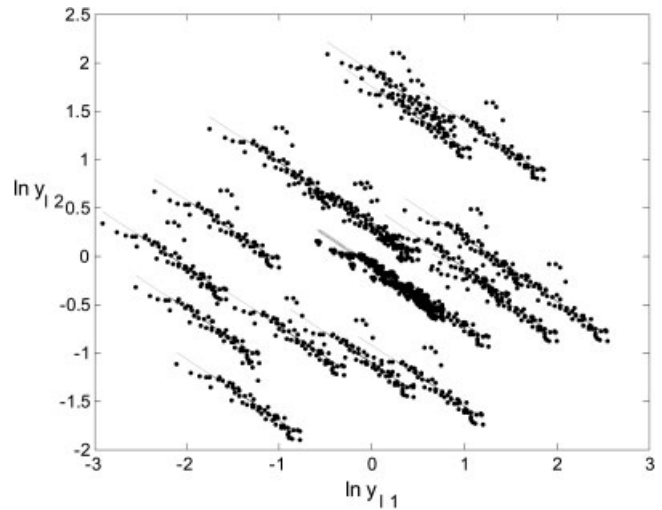


FIG. 1. Representation of logarithm  $y_{\lambda_2}$  versus logarithm  $y_{\lambda_1}$  for the monochromatic sensors situated at 450, 610, and 540 nm.

been found to be more linear with regard to visual perception.<sup>15,16</sup> Furthermore, other authors<sup>7,9</sup> have measured daylight SPDs with color temperatures of more than 20 000 K when the sun was near to or even below the horizon (twilight).

Initially we chose as our narrow-band sensors those used by Finlayson and Hordley,<sup>2</sup> corresponding to wavelengths of  $\lambda_1 = 450$  nm,  $\lambda_2 = 610$  nm, and  $\lambda_n = 540$  nm. Using these sensors we calculated the values of  $1/A_{12}$  by two different methods and compared them with the values with the graphs of the logarithm  $y_{\lambda_2}$  versus that logarithm  $y_{\lambda_1}$ . The first method was a repeat of Marchant and Onyango's<sup>4</sup> calculation, which involves carrying out a PCA on the logarithms of the values of the daylight SPDs arrived at by the CIE approach. The second method was similar to the first, but using our 2600 experimental daylight data<sup>9</sup> to obtain the basis. We tested the validity of the methods by comparing the calculated values of  $1/A_{12}$  with that deriving from the graphic representations. To define this value we took as our objects 24 samples from the ColorChecker and 64 daylight SPDs corresponding to measurements taken on days with diverse atmospheric conditions and at different times of day: 22 daylight (direct sunlight + skylight) at intervals of 10 mireds, 21 skylight, and 21 twilight at the same intervals. An example of the representations carried out is shown in Fig. 1. We constructed a straight line for each object, the correlation coefficients of which are around 0.887, despite which their slopes are practically the same for all the objects at  $-0.634$ .

The values of  $1/A_{12}$  obtained by the two methods are  $-0.483$  and  $-0.776$ , respectively. These values are clearly different from the value obtained graphically, although the use of our own of eigenvectors (second method) leads to a slightly closer result to the graphical value. The discrepancies between calculated and graphical values are mainly due to the use of only one eigenvector in the linear model of representation of daylight SPD. We can conclude that the

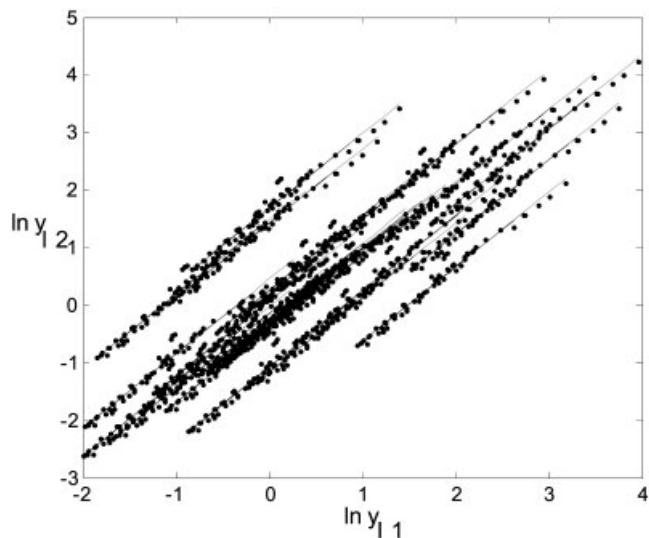


FIG. 2. Representation of logarithm  $y_{\lambda_2}$  versus logarithm  $y_{\lambda_1}$  for the monochromatic sensors situated at 550, 610, and 400 nm.

calculation of the invariant, based on a linear model with only one degree of freedom, is not useful when daylight is involved.

#### SEARCH FOR OPTIMUM SENSORS

We applied an exhaustive-search method so as to find the optimum set of three narrow-band sensors to represent the results for the 24 objects of the ColorChecker and 64 daylight SPDs. To this end we developed a program that would locate the three monochromatic sensors in all their possible spectral positions within the visible range (400–700 nm) and evaluate the quality of the invariant obtained for the whole set of 24 objects and 64 illuminants. The best results, when a minimum of 50 nm of difference between wavelength was imposed, were given by the sensors  $\lambda_1 = 550$  nm,  $\lambda_2 = 610$  nm, and  $\lambda_n = 400$  nm. The results obtained for different objects in the graph of logarithm  $y_{\lambda_2}$  versus logarithm  $y_{\lambda_1}$  are shown in Fig. 2. For the three monochromatic sensors in question the slopes are the same for all the objects (1.295) and all the correlation coefficients work out at 0.989. Thus we can be confident that the behavior of the experimental invariant is excellent for these sensors.

Previously, we found even better results with the sensors  $\lambda_1 = 645$  nm,  $\lambda_2 = 675$  nm, and  $\lambda_n = 595$  nm, when a minimum of 30 nm of difference between wavelength peaks was imposed in the exhaustive search. This set of sensors, despite not covering the short-wavelength region in the visible spectrum, still afforded excellent results for blue objects from the ColorChecker due to the wide spectral reflectances of these samples. This result is not unexpected, since in agreement with the definition of the invariant, the best results are expected for sensors which are very close to each other. Anyway, we found essential to cover appropriately the visible spectrum with the three sensors centered in

the short, medium, and long-wavelength regions respectively. For this reason, we have not considered this nonrealistic set of sensors in the rest of our analysis.

The results obtained graphically using five triads of monochromatic sensors are set out in Table I. The data include the triad which afforded the best results with a minimum separation of 50 nm between sensors (second row), the triad used by Finlayson and Hordley<sup>2</sup> (third row), and a triad quite close to that used by Marchant and Onyango<sup>1</sup> (fourth row). We also applied the exhaustive-search method to obtain the best triad of sensors which optimize at the same time entropy, range, and correlation coefficients of the data shown as in Figs. 1 and 2. In this case the best triad found is (545, 605, and 435 nm) and the results shown in the fifth row. As these wavelength are very close to that proposed by Finlayson and Funt<sup>17</sup> and employed by Finlayson and Hordley<sup>2</sup> we have also tested these last sensors but in a different way, that is being  $\lambda_n = 450$  nm. Then the results of the Finlayson and Hordley modified triad appear in the sixth row of Table I. The typical deviations of the different slope values have not been included because they were negligible. It can be seen that the triads of sensors found with the exhaustive search give improved results compared to those obtained with the rest of the sensors in that the average correlation coefficient is better, showing values that fit satisfactorily to a linear regression. Nevertheless, results for the rest of triads of sensors, with the exception of nonmodified Finlayson and Hordley sensors, can be also considered quite good and invited us to further tests of their behavior when natural color images are analyzed.

This study serves to present the good results generated for daylight by the invariant defined in Eq. (1). As can be seen, given a natural scene for which we know the values of the response to this type of sensor pixel by pixel, we can reliably find a descriptor that is invariant to changes in

TABLE I. Values of the average slope and correlation coefficient and  $A_{12}$  obtained by the graphical method for monochromatic sensors with maximum spectral sensitivities at  $\lambda_1$ ,  $\lambda_2$ , and  $\lambda_n$ .

Wavelength (nm) $\lambda_1, \lambda_2, \lambda_n$	Average slope	Average correlation coefficient	$A_{12}$
550 610 400	1.295	0.989	0.772
450 610 540	-0.634	0.887	-1.578
605 530 440	0.562	0.977	1.778
545 605 435	1.474	0.984	0.678
540 610 450	1.634	0.980	0.612

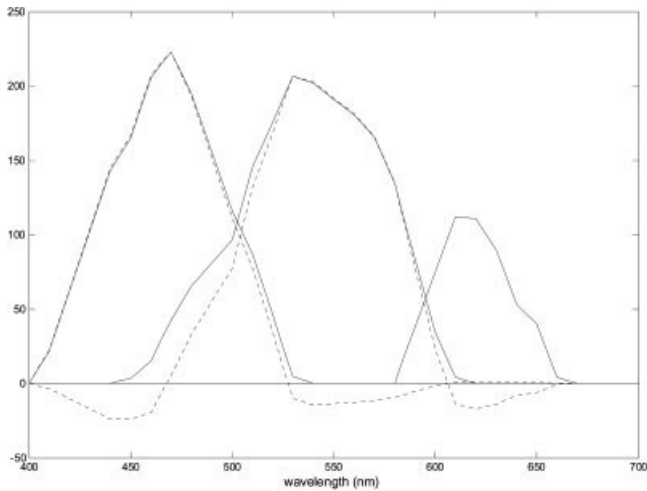


FIG. 3. Spectral sensitivities of the JVC TK-1270 E CCD camera sensors (solid lines) and sharpened sensors (dashed lines).

daylight illumination. That is to say, we can translate it to a scene in the grey scale, in which shadows disappear and the objects can be chosen according to the value of  $F_{12}$ . Object-recognition experiments based on this premise have been made by other authors<sup>1,2</sup> with satisfactory results when all that is required is, for example, to eliminate shadows so as to be able to distinguish between vegetation and soil<sup>1</sup> or to recognize artificial objects under different types of illuminants.<sup>2</sup> In our case we are interested in applying these results to natural scenery so as to classify different types of vegetation. Before doing this, however, it would be interesting to see whether our study might be widened to include the use of wide-band sensors close to real ones, or to the real sensors of a commercial CCD camera, which we do in the following section.

#### WIDE-BAND-SENSITIVITY SENSORS

When the logarithm  $y_{\lambda_2}$  is represented graphically versus logarithm  $y_{\lambda_1}$  for a set of sensors centered on the wavelengths that afforded the best results in the section above, but giving them Gaussian spectral sensitivity with a band width half that of the 30-nm peak, the results do not differ from those shown in Fig. 2. The adjusted straight lines show an excellent correlation coefficient for all the objects. These results confirm the satisfactory behavior of this type of sensor when applied to daylight, and thus we believe, to images taken of natural scenery.

We also used sensors belonging to a commercial CCD camera (JVC TK-1270E CCD) (Fig. 3, solid lines). The behavior of these sensors did not turn out so well as those in the former simulations (Fig. 4). The correlation coefficients were somewhat worse, although always higher than 0.960, and the differences between slopes showed a maximum of  $12.62^\circ$ , which are about the same as the values found by Finlayson and Hordley<sup>2</sup> in representations of this kind.

The values obtained, for the different sets of Gaussian

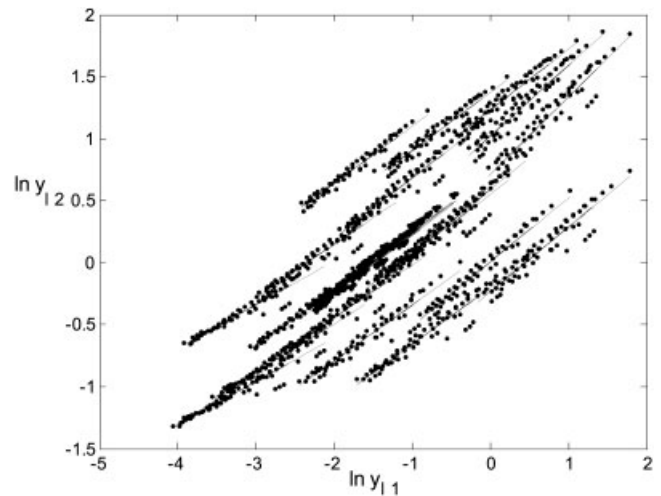


FIG. 4. Representation of logarithm  $y_{\lambda_2}$  versus logarithm  $y_{\lambda_1}$  for the sensors of the commercial CCD camera shown in Fig. 3.

sensors and CCD sensors, for  $A_{12}$  and the mean correlation coefficients from the graphic representations are set out in Table II. These results for the Gaussian sensors are very similar to those obtained for monochromatic sensors with maximum sensitivity in the same wavelength (Table I), the values of the correlation coefficients being practically the same as those produced by monochromatic sensors. They are slightly worse in that the definition of the invariant changes slightly according to the object in question, i.e., the value of the slope of the adjusted straight line for each object shows a noticeable typical deviation. The results for

TABLE II. Values of average slope and correlation coefficient and  $A_{12}$  obtained by the graphical method for 30-nm bandwidth Gaussian sensors with maximum spectral sensitivities at  $\lambda_1$ ,  $\lambda_2$ , and  $\lambda_n$  and CCD camera sensors.

Wavelength (nm) $\lambda_1, \lambda_2, \lambda_n$	Average slope <sup>a</sup>	Average correlation coefficient	$A_{12}$
550 610 400	1.320(0.017)	0.989	0.758
450 610 540	-0.617(0.037)	0.892	-1.617
605 530 440	0.563(0.017)	0.978	1.776
545 605 435	1.443(0.026)	0.987	0.693
540 610 450	1.619(0.037)	0.982	0.618
CCD	0.467(0.059)	0.964	2.135

<sup>a</sup> Values in parentheses indicate  $\sigma$  values.



FIG. 5. Image of a natural scene (Nascimento *et al.*<sup>18</sup>) in shades of grey after applying the invariant parameter.

the CCD sensors are clearly worse than those obtained for the rest of triads with the exception of that based on Finlayson and Hordley.<sup>2</sup>

Thus in the following section we investigate the influence that these small variations might have on object recognition by studying the histograms of images in the grey-scale

obtained by assigning the value of  $F_{12}$  to each pixel of a color image.

#### APPLICATION TO NATURAL IMAGES

To test the behavior of the invariant and sensors in object-recognition tasks we chose one of the multispectral images provided by Nascimento *et al.*,<sup>18</sup> which they catalogue as a natural scene. In Fig. 5 we show this image translated into the grey-scale by applying the invariant. The idea is to see whether this method will allow us to distinguish between flowers and other types of vegetation such as leaves, which could also be applied to recognizing ripe fruit against a green background. In Figs. 6(a)–6(e) we show the histograms deriving from the grey-scale images produced by five sets of nonmonochromatic sensors studied above (cf. Table II). All the histograms show bimodal distributions, which correspond to two main kinds of vegetation in the image: flowers and leaves. Nevertheless, the sensors behave in different ways when these distributions are obtained during different phases of daylight. Thus we obtained the histograms for six daylight SPDs<sup>9</sup> with color temperatures of 3757, 4425, 5555, 9091, 12 449, and 32 753 K, equally spaced in the mired scale, corresponding to daylight phases in clear and cloudy weather and during twilight. As can be seen for the set of Gaussian sensors with 30-nm bandwidth and maxima in the wavelengths of 550, 610, and 400 nm [Fig. 6(a)], the histograms are approximately juxtaposed

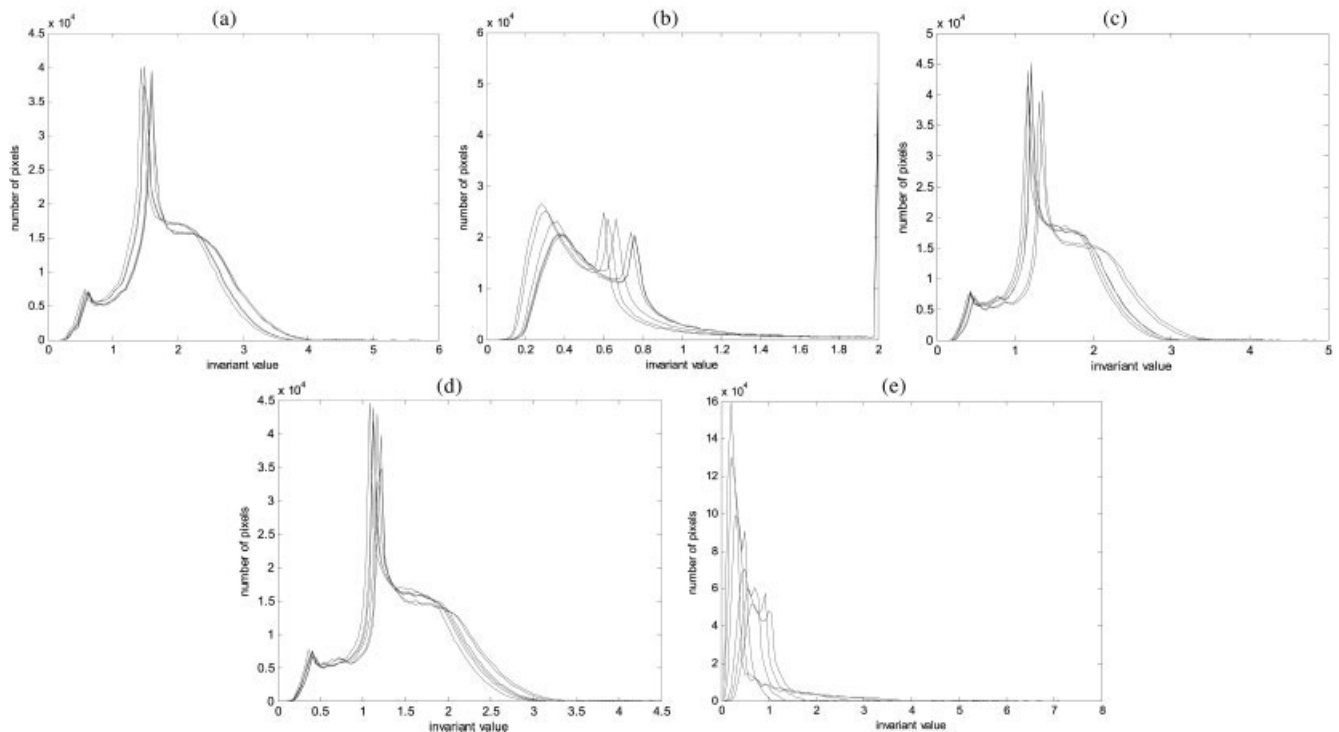


FIG. 6. Histograms of the image in Fig. 5 obtained for six daylight SPDs: (a) Gaussian sensors with maximum spectral sensitivities at  $\lambda_1 = 550$ ,  $\lambda_2 = 610$ , and  $\lambda_n = 400$  nm; (b) Gaussian sensors with maximum spectral sensitivities at  $\lambda_1 = 605$ ,  $\lambda_2 = 530$ , and  $\lambda_n = 440$  nm; (c) Gaussian sensors with maximum spectral sensitivities at  $\lambda_1 = 545$ ,  $\lambda_2 = 605$ , and  $\lambda_n = 435$  nm; (d) Gaussian sensors with maximum spectral sensitivities at  $\lambda_1 = 540$ ,  $\lambda_2 = 610$ , and  $\lambda_n = 450$  nm; (e) Sensors of the commercial CCD camera (cf. Fig. 3).



FIG. 7. Example of segmentation for the natural image analyzed (Fig. 5) and the (550, 610, and 400 nm) Gaussian sensors.

and so the task of recognition is possible whatever the illuminant. The results are not as good for other sensors, but leading us to deduce that it would be possible to recognize flowers against a background of leaves for some triads of sensors because the two peaks in the histograms are clearly separated. To evaluate this, we compared the maximum difference among histograms in the invariant value for each peak and the minimum distance between peaks, which is the difference, in terms of the value of the invariant, between the first peak most at right and the second peak most at left. As an example, in Fig. 6(a) these differences are 0.171 (maximum difference among histograms peaks) and 0.801 (minimum distance between different peaks) respectively. If we assume that the first difference must be less than the second in at least three times to obtain clearly grouped histograms, we can conclude that the Gaussian sensors with maximum sensitivity in (550, 610, and 400 nm), (545, 605, and 435 nm), and (540, 610, and 450 nm) could be used to the recognition task proposed. This conclusion is strengthened when daylight SPD corresponding to central hours of the day are studied apart from twilight (higher correlated color temperature). Figure 7 shows an example of segmentation for the natural image analyzed and the (550, 610, and 400 nm) Gaussian sensors, where flowers are distinguished from leaves.

The results for the sensors in the CCD camera are not so good [Fig. 6(e)]. To improve on these results we decided to resort to one of the techniques proposed to achieve better applicability of these systems to the task of object recognition.<sup>11-13</sup> Thus we carried out a spectral sharpening on the CCD camera sensors using the L2-L2 technique suggested by Drew and Finlayson,<sup>19</sup> this being one of the techniques which afford the best results. Although this method may produce negative values in the sensitivities transformed from the original sensors, these values do not generate

negative R, G, B values when calculated for the objects and illuminants in question. The spectral sensitivities of the sensors transformed by spectral sharpening are shown in Fig. 3 (dashed lines).

The histograms derived from the sharpened sensors are shown in Fig. 8. The results show an improvement on those obtained before with the CCD camera sensors [Fig. 6(e)], although they are still not comparable to those obtained with the best sets of Gaussian sensors [Figs. 6(a), 6(c), and 6(d)]. There is a clear improvement in the results obtained with the CCD sensors, but we cannot conclude that these sensors allow any recognition of objects invariant to changes in daylight comparable to that which can be achieved with some of the other sets of sensors analyzed.

## CONCLUSIONS

As we have mentioned, the definition of a pixel-by-pixel invariant of an image refers to its application to the recognition of objects invariant to changes in illumination whenever certain conditions that affect both the characteristics of the illuminants and the type of sensors used in the system hold good. We have carried out this optimization on the base of real daylight measurements taken at extremely diverse elevations of the sun from dawn to dusk, including twilight hours (high color temperatures). The calculations of the invariant, made via the determination of the parameter  $A_{12}$ , can be replaced by the graphical determination according to the graphs shown in Figs. 1 and 2, which are obtained by calculating the responses of the sensors to the light reflected by different objects illuminated by different illuminants. This method has allowed us, by using an exhaustive-search technique, to obtain the position of the wavelengths corresponding to triads of monochromatic sensors, which give better results in obtaining the invariant. Thus we found that the triad of sensors with maximum spectral

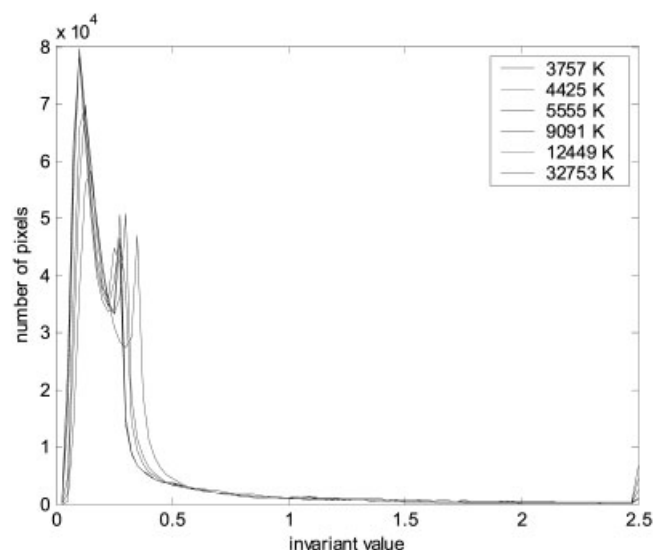


FIG. 8. Histograms of the image in Fig. 5 obtained for six daylight SPDs and the sharpened sensors of the commercial CCD (cf. Fig. 3).

sensitivities at (550, 610, and 400 nm) afforded excellent results. In addition, results for the triads (545, 605, and 435 nm), and (540, 610, and 450 nm) were also excellent, the first triad obtained by optimizing the entropy, range, and correlation coefficient simultaneously and the second by reordering Finlayson and Funt<sup>17</sup> proposed sensors.

When we take into consideration sensors with spectral sensitivity of a certain bandwidth, the Gaussian sensors with a 30-nm bandwidth and wavelengths at the maximum in the triad of values mentioned above also allow a satisfactory application of the invariant, much better than that afforded by the sensors of a commercial CCD camera. We have put this to the test in two ways: first, by calculating the invariant graphically (cf. Table II), and second, by applying the invariant to a natural scene. As far as this scene is concerned, by applying the invariant we can obtain a grey-scale image for each illuminant, which should remain the same when the illuminant changes. When the best Gaussian sensors are analyzed, the histograms of the values of the invariant approximately superimpose one upon the other, but this does not apply to some of the other sets of sensors analyzed. When we attempted to improve the possibilities of applying a CCD camera to the task of object recognition by using the spectral-sharpening technique to narrow the sensitivities of the camera's sensors and so bring them closer to the ideal conditions for the application of the invariant, we could not achieve better results than those obtained with the Gaussian sensors with maximum sensitivities in the triad of wavelength mentioned above. It may be feasible, according to present-day technology in cameras and LCTF filters, to implement experimentally this type of sensor.

#### ACKNOWLEDGMENTS

The authors thank Prof. Sergio Nascimento for comments and suggestions.

1. Marchant JA, Onyango CM. Shadow-invariant classification for scenes illuminated by daylight. *J Opt Soc Am A* 2000;17:1952–1961.
2. Finlayson GD, Hordley SD. Color constancy at a pixel. *J Opt Soc Am A* 2001;18:253–264.
3. Marchant JA, Onyango CM. Color invariant for daylight changes: Relaxing the constraints on illuminants. *J Opt Soc Am A* 2001;18:2704–2706.
4. Marchant JA, Onyango CM. Spectral invariance under daylight illumination changes. *J Opt Soc Am A* 2002;19:840–848.
5. Judd DB, MacAdam DL, Wyszecki G. Spectral distribution of typical daylight as a function of correlated colour temperature. *J Opt Soc Am* 1964;54:1031–1041.
6. CIE. Colorimetry. CIE Technical Report No. 15.2. Central Bureau of the CIE, Vienna; 1986. pp 70–72.
7. Dixon ER. Spectral distribution of Australian daylight. *J Opt Soc Am* 1978;68:437–450.
8. Slater D, Healey G. Analyzing the spectral dimensionality of outdoor visible and near-infrared illumination functions. *J Opt Soc Am A* 1998;15:2913–2920.
9. Hernández-Andrés J, Romero J, Nieves JL, Lee RL, Jr. Color and spectral analysis of daylight in southern Europe. *J Opt Soc Am A* 2001;18:1325–1335.
10. Finlayson GD. Spectral sharpening: What is it and why is it important? Proceedings of the First European Conference on Colour in Graphics, Imaging and Vision, Poitiers, France, 2002. pp 230–235.
11. Finlayson GD, Drew MS, Funt BV. Spectral sharpening: Sensor transformations for improved color constancy. *J Opt Soc Am A* 1994;5:1553–1563.
12. Finlayson GD, Drew MS. 4-Sensor camera calibration for image representation invariant to shading, shadows, lighting and specularities. Proceedings of the International Conference on Computer Vision, Vancouver, Canada, 2001. pp 473–480.
13. Drew MS, Chen C, Hordley SD, Finlayson GD. Sensor transforms for invariant image enhancement. Proceedings of the 10th Color Imaging Conference, Scottsdale, Arizona, 2002. pp 325–329.
14. Thomson MGA, Westland S. Color-imager calibration by parametric fitting of sensor responses. *Color Res Appl* 2001;26:442–449.
15. Tominaga S, Wandell BA. Natural scene-illuminant estimation using the sensor correlation. *Proc IEEE* 2002;90:42–56.
16. Wyszecki G, Stiles WS. *Color Science: Concepts and Methods, Quantitative Data and Formulae*. New York: Wiley; 1982. pp 224–225.
17. Finlayson GD, Funt BV. Coefficient channels: Derivation and relationship to other theoretical studies. *Color Res Appl* 1996;21:87–96.
18. Nascimento SMC, Ferreira FP, Foster DH. Statistics of spatial cone-excitation ratios in natural scenes. *J Opt Soc Am A* 2002;19:1484–1790.
19. Drew MS, Finlayson GD. Spectral sharpening with positivity. *J Opt Soc Am A* 2000;17:1361–1370.